White-light whispering gallery mode resonances in optically levitated aerosol droplets

Contact andy.ward@stfc.ac.uk

A. D. Ward and O. Hunt
Central Laser Facility, STFC, Rutherford Appleton Laboratory, HSIC, Didcot, Oxon, OX11 0QX, UK

M. Zhang
Cornell University, Ithaca, NY 1485, USA

Introduction

Understanding the behaviour of aerosols underpins a number of scientific disciplines including atmospheric science, engine combustion and drug delivery. In the study of aerosols, the basic chemical and physical properties, such as droplet size, refractive index, evaporation dynamics and chemical compositions are of great importance[1,2]. The optical levitation of individual aerosol droplets is a well-established technique that is increasingly used in these studies and provides the advantage of a non-intrusive and precise means of aerosol manipulation and characterisation[3-8].

Here we describe a simple and efficient means of using an LED-based white light broadband source for droplet property characterisation in combination with optical levitation. The technique provides high resolution (0.1 nm) Mie scattering intensity distributions across a spectral range of 480-700 nm. The experimental data provides sufficient information to allow assignment of resonance mode numbers and mode orders from conventional Mie theory calculations. The calculations are made assuming a conical collection volume, dependent on the numerical aperture of the objective lens, in a 180 degree backscattering geometry. Refractive index dispersion can be determined from a single refractive index value at known wavelength.

Theory

The unique resonance structure in both elastic and inelastic scattering by aerosols is commonly referred to as Whispering Gallery Mode (WGM)[1,4,9] or Morphology-Dependent Resonances (MDR)[10-13]. It can be understood as light rays circling around a droplet via total internal reflection at the liquid-air interface. When the wavelength of the light matches a resonance mode of the cavity, two counter propagating waves form a standing wave around the droplet. For each resonance mode, a mode number n is commonly used to describe the number of maxima around the circumference of the cavity. A mode order l is employed to specify the number of maxima existing in radial intensity dependence. The resonance mode can be a Transverse Electric (TE) mode or a Transverse Magnetic (TM) mode. A TE mode has no radial dependence on the electric component of the field and a TM mode has no radial dependence on the magnetic component of the field[1]. Mie theory provides analytical descriptions for the intensity of the electromagnetic field scattered by mesoscopic particles.

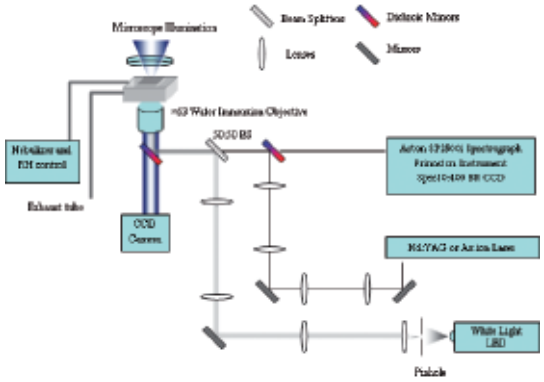

Figure 1. A schematic diagram of the experimental setup.

Sizing of the droplet thus requires fitting of experimental scattering data to theoretical positions of Mie scattering coefficients calculated using the relative refractive index dispersion of the droplets to the surrounding media across the spectral range[14,15].

Experimental

A schematic diagram of the experimental setup is shown in Figure 1. We have used two separate laser systems for optical trapping of droplets. These were (i) a cw Nd:YAG laser (Laser 2000) operating at its fundamental frequency (1064 nm) and (ii) a cw Ar-ion laser (Coherent Innova 308C) operating at 514.5 nm.

The trapping laser beam is directed into an inverted microscope (Leica, DM-IRB) and reflected by a dichroic mirror (CVI Technical Optics Ltd) to be focussed using a ×63 water immersion objective with numerical aperture of 1.2. The trapping power was 2 mW for 1064 nm and 10 mW for 514.5 nm. A similar setup is employed for the broadband LED white light source (Comar 6V, 20 mA, 3.0 cd). The LED light is directed into the microscope using broadband 50:50 beam splitter and is focused with the same objective as for the trapping laser. A pin hole is placed in a focal plane of the LED optical path, such that an image of the pinhole is formed at the optical focus, parfocal with the laser trap and the optical microscope imaging plane. The size of this spot is 10 µm as imaged and measured using the microscope. Backscattered light is collected with the same optics and is directed to a spectrograph (Acton SP2500i) and CCD (Princeton Instrument Spec10:400 BR). Spectra are collected from a 1200 groove/mm grating to resolve fine

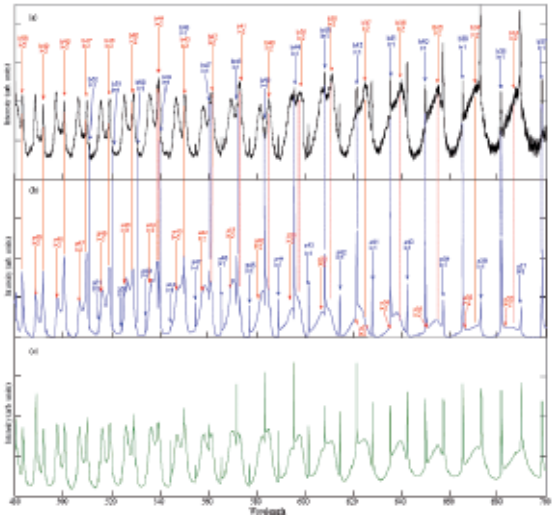

Figure 2. Spectral data of the whispering gallery mode resonances comparing experimentally acquired data (a) to that of theoretical predictions (b) and (c) using sharp resonance peaks to accurately model to droplet size and refractive index.

resonance structures. The spectrograph and CCD were calibrated across the spectral range using a Hg:Ne discharge lamp to an accuracy of 0.03 nm. The spectrograph slit width was 15 microns.

Aerosol droplets, generated by an ultrasonic nebuliser (Aerosonic), are pumped into an enclosed aerosol cell which is mounted on the microscope. Once a droplet is trapped the nebuliser is turned off. A mass flow control unit provides a saturated environment in the cell by means of passing dry nitrogen through water. A 20 gl^{-1} sodium chloride solution was used to produce the droplets. The presence of sodium chloride allows the droplets to be stable and trapped for hours in this saturated environment [4]. Stable trapping of droplets of 1-8 microns in radius is achieved. The ambient temperature of the laboratory was 22 ºC.

Results

Figure 2(a) shows the experimentally obtained resonance peaks for a droplet. The spectrum consists of seven contiguous spectra produced by scanning the grating across the wavelength range. First order resonances are apparent at longer wavelengths, although these become difficult to resolve at shorter wavelengths. An estimate of the droplet size is first calculated from the spacing of the resonance modes and the microscope images (Fig. 3).

The refractive index dispersion was assumed a priori to be that of a 20 gl^{-1} salt solution and the dispersion relation, calculated using the algorithm reported by Millard and Seaver [16], is then used in generating a series of theoretical scattered spectrum. The theoretical spectra are varied for droplet sizes within ±10% of the estimated size (3.50 ± 0.35 microns) until a best fit of the experimental resonance peaks is obtained as shown in Fig 2. At the optimum radius, 3.523 microns, the average distance between experimental and theoretical peaks was found to be less than 0.1 nm.

The theoretical resonances were calculated assuming a 180° backscattering geometry. The calculations

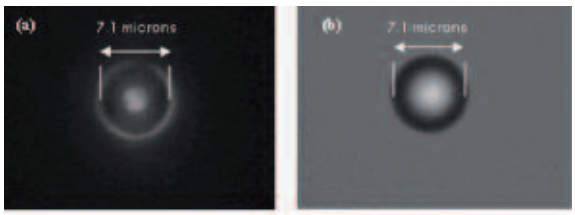

Figure 3. Images taken of the same optically trapped water droplet showing the droplets with (a) white-light plane wave illumination and (b) under standard illumination. The droplet size accurately determined by resonance positions is slightly lower than that using optical imaging.

generate satisfactory peak positions but the scattering intensity distribution was not ideal. The illumination geometry as described is unusual for Mie scattering studies as the light source is focused with a cone angle approaching 60° from the objective lens. Thus, whilst scattered light is collected in a 180° backscattering geometry, there are Mie scattered light contributions that originate from all angles within this cone. The overall effect is analogous to integrating the Mie scattered light over a definite solid acceptance angle around the backscattered direction [17]. The best fit for the scattered intensity distribution is for integration between 120° and 180° as shown in Fig. 2(c). Such a fit significantly improves the intensity distribution from that of 180° backscattering geometry whilst the resonance positions are identical.

Calculated TM and TE modes are assigned in Figs. 2(a) and 2(b). The assignment shows that the narrow peaks between 540 nm and 700 nm are first order resonances (l=1). As wavelength decreases, the lowest order resonances become increasingly narrow and eventually cannot be resolved by the spectrometer. The narrowest peak observed (a48,1) shows a FWHM of approximately 0.1 nm.

Changes in the droplet size of less than a nanometer can lead to a shift of the calculated resonance modes which are readily discernable when compared to the experimentally obtained spectrum. However, due to the limitation of the CCD resolution, we estimate the error in droplet sizing is within 2 nm. The size range, for which an accuracy of 2 nm applies, is dependent on the presence of narrow, first order peaks which provide the most stringent test of fitting quality. For water based droplets, with which we are primarily concerned with in this study, the first order resonances will not be discernable when the radius is below 2 µm. At above 10 µm radius it will become difficult to clearly resolve the resonance positions, although there is a further practical caveat to this in that only droplets of radius 1 µm to 8 µm can be optically trapped. Thus, the practical size range for the application of this methodology is 2 µm to 8 µm for water based droplets. This range will decrease to lower sizes as refractive index increases. Analyzing the images of the droplet acquired from the CCD camera in the microscope (Fig. 3) shows the droplet size calculated from Mie scattering is slightly below that imaged by the camera under brightfield illumination [18].

A single refractive index at known wavelength can be used to match theoretical and experimental scattering data. For example, using a fixed refractive index of

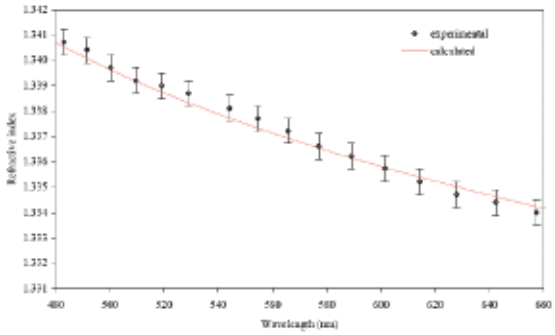

Figure 4. Dispersion relation obtained from matching of the Mie resonance peaks and calculated using the algorithm reported by Millard *et al.*

1.3360 at 598 nm, the refractive index of 20 gl^{-1} saltwater at room temperature[19], we align the first order resonance peak near 598 nm by varying droplet size within ±1 % of the calculated size. The sequential resonance modes at other wavelengths are then aligned by assuming constant size and adjusting refractive index. In this way the dispersion relation can be experimentally obtained as shown in Fig. 4. Comparing the dispersion relation obtained with this method and with the dispersion relation calculated using Millard's algorithm[16] suggests broadband Mie resonances can be used for determining the refractive index dispersion of the droplet.

Conclusions

The technique has a wide range of potential applications, including the study of droplet deformation and droplet coagulation, as resonances are sensitive to droplet shape[20]. Since temperature and refractive index are correlated, the technique can also be developed for temperature measurement of mesoscopic dielectric spheres including particles and emulsions in solution. Finally, absorption of resonating light by molecules within the droplets, or at the air/water interface, can significantly alter Mie scattering intensities, a feature which could be used to follow photochemistry and heterogeneous surface chemistry.

Acknowledgments

We would like to thank the Science and Technologies Facility Council for providing funding through the Strategic Initiative Programme Grant (HS30635). This article is based upon original material by A. D. Ward, O. Hunt and M. Zhang, *Optics Express*, Vol. 16 Issue 21 pp. 16390-16403 (2008) doi: 10.1364/OE.16.016390.

References

1. R. Symes, R. M. Sayer, and J. P. Reid "Cavity enhanced droplet spectroscopy: Principles, perspectives and prospects," *Phys. Chem. Chem. Phys*. **6**, 474-487 (2004).
2. J. H. Seinfeld and S. N. Pandis, *Atmospheric Chemistry and Physics: From Air Pollution to Climate Change* (New York, Wiley, 1998).
3. A. Ashkin, J. M. Dziedzic, J. E. Bjorkholm, and S. Chu, "Observation of a single-beam gradient force optical trap for dielectric particles," *Opt. Lett*. **11**, 288 (1986).
4. L. Mitchem and J. P. Reid "Optical manipulation and characterisation of aerosol particles using a singlebeam gradient force optical trap," *Chem. Soc. Rev*. **37**, 756-769 (2008).
5. D. McGloin, "Optical Tweezers: 20 years on," *Philos. Trans. R. Soc. A* **364**, 3521-3527 (2006).
6. D. McGloin, D. R. Burnham, M. D. Summers, D. Rudd, N. Dewar, and S. Anand, "Optical manipulation of airborne particles: techniques and applications," *Faraday Discuss*. **137**, 335-350 (2008).
7. K. Dholakia, P. Reece, and M. Gu, "Optical micromanipulation," *Chem. Soc. Rev*. **37**, 42-55 (2008).
8. M. D. King, K. C. Thompson, and A. D. Ward, "Laser Tweezers Raman Study of Optically Trapped Aerosol Droplets of Seawater and Oleic Acid Reacting with Ozone: Implications for Cloud-Droplet Properties," *J. Am. Chem. Soc*. **126**, 16710-6711 (2004).
9. A. A. Zardini, U. K. Krieger, and C. Marcolli "White light Mie resonance spectroscopy used to measure very low vapor pressures of substances in aqueous solution aerosol particles," *Opt. Express* **14**, 6951-6962 (2006).
10. J. B. Snow, S. Qian, and R. K. Chang "Stimulated Raman scattering from individual water and ethanol droplets at morphology-dependent resonances," *Opt. Lett*. **10**, 37 (1985).
11. R. Pastel and A. Struthers, "Measuring Evaporation Rates of Laser-Trapped Droplets by Use of Fluorescent Morphology-Dependent Resonances," *Appl. Opt*. **40**, 2510-2514 (2001).
12. P. Chylek "Absorption effects on microdroplet resonant emission structure," *Opt. Lett*. **16**, 1723 (1991).
13. A. B. Matsko, A. A. Savchenkov, R. J. Letargat, V. S. Ilchenko and L. Maleki, "On cavity modification of stimulated Raman scattering," *J. Opt. B Quantum Semiclassical Opt*. **5**, 272-278 (2003).
14. P. Chylek "Resonance structure of Mie scattering: distance between resonances," *J. Opt. Soc. Am. A* **7**, 1609-1613 (1990).
15. A MATLAB program is employed using the algorithm described by Bohren and Huffman.
16. R. C. Millard and G. Seaver, "An index of refraction algorithm for seawater over temperature, pressure, salinity, density, and wavelength," *Deep-Sea Res*. **37**, 1909-1926 (1990).
17. P. Chylek, V. Ramaswamy, A. Ashkin and J. M. Dziedzic, "Simultaneous determination of refractive index and size of spherical dielectric particles from light scattering data," *Appl. Opt*. **22**, 2302-2307 (1983).
18. K. J. Knox, J. P. Reid, K. L. Hanford, A. J. Hudson and L. Mitchem, "Direct measurements of the axial displacement and evolving size of optically trapped aerosol droplets," *J. Opt. A: Pure Appl. Opt*. **9**, S180–S188 (2007).
19. D. R. Lide, ed., CRC Handbook of Chemistry and Physics 88th Edition, (Boca Raton, FL, Taylor and Francis, 2007).
20. I. Mishchenko and A. A. Lacis, "Morphology-dependent resonances of nearly spherical particles in random orientation," *Appl. Opt*. **42**, 5551-5556 (2003).